BioResearch Open Access
Volume 2, Number 5, October 2013

DOI: 10.1089/biores.2013.0031

Biofabrication Under Fluorocarbon: A Novel Freeform Fabrication Technique to Generate High Aspect Ratio Tissue-Engineered Constructs

Andreas Blaeser,[1,2] Daniela F. Duarte Campos,[2] Michael Weber,[2] Sabine Neuss,[1,3] Benjamin Theek,[4] Horst Fischer,[2] and Willi Jahnen-Dechent[1]

Abstract

Bioprinting is a recent development in tissue engineering, which applies rapid prototyping techniques to generate complex living tissues. Typically, cell-containing hydrogels are dispensed layer-by-layer according to a computer-generated three-dimensional model. The lack of mechanical stability of printed hydrogels hinders the fabrication of high aspect ratio constructs. Here we present submerged bioprinting, a novel technique for freeform fabrication of hydrogels in liquid fluorocarbon. The high buoyant density of fluorocarbons supports soft hydrogels by floating. Hydrogel constructs of up to 30-mm height were generated. Using 3% (w/v) agarose as the hydrogel and disposable syringe needles as nozzles, the printer produced features down to 570-μm diameter with a lateral dispensing accuracy of 89 μm. We printed thin-walled hydrogel cylinders measuring 4.8 mm in height, with an inner diameter of $\sim$2.9 mm and a minimal wall thickness of $\sim$650 μm. The technique was successfully applied in printing a model of an arterial bifurcation. We extruded under fluorocarbon, cellularized alginate tubes with 5-mm outer diameter and 3-cm length. Cells grew vigorously and formed clonal colonies within the 7-day culture period. Submerged bioprinting thus seems particularly suited to fabricate hollow structures with a high aspect ratio like vascular grafts for cardiovascular tissue engineering as well as branching or cantilever-like structures, obviating the need for a solid support beneath the overhanging protrusions.

Keywords: biomaterials; cardiology; cell culture; tissue engineering

Introduction

Classical tissue engineering combines three elements: cells, biomaterial scaffolds, and molecular signals.[1] Cells are seeded on or within a biomaterial scaffold and are cultured in complex media containing with biological and chemical cues.[2–4] Until now, primarily thin and avascular tissues like cartilage or skin could be generated with this approach.[5,6] Two major obstacles prevent the engineering of high aspect ratio, complex tissue constructs. First, the limited diffusion capabilities of oxygen, carbon dioxide, and nutrients limit the potential thickness of tissue-engineered constructs. Tissues thicker than $\sim$1 mm require vascularization for cell survival.[7,8] Another shortcoming of conventional tissue engineering is the lack of precision in cell placement, which prevents the direct fabrication of complex, multicellular tissues.[9]

Bioprinting is an emerging technique, which may overcome these limitations by generating three-dimensional (3D) living tissues using fabrication technology originally developed for rapid prototyping.[10–12] In a typical bioprinting approach, cell-containing hydrogels are dispensed layer-by-layer to form cellular constructs of predefined morphology.[13,14] Ideally, scaffold materials used for bioprinting should mimic the extracellular matrix of living tissue and should provide mechanical as well as biological cues.[15–19] Hydrogels are particularly suitable as bioprinting materials, because their elasticity and polymerization time can be controlled by varying the amount of cross-linking agent, pH value, or temperature.[16,20–22] However, the weak mechanical properties of hydrogels used in bioprinting impede fabrication of macroscopic scaffolds on a centimeter or decimeter scale.[19,23,24] Tissue constructs with a high aspect ratio usually collapse under

[1]Biointerface Laboratory and [4]Experimental Molecular Imaging, Helmholtz Institute of Biomedical Engineering; [2]Department of Dental Materials and Biomaterial Research; [3]Institute of Pathology; RWTH Aachen University Hospital, Aachen, Germany.

ABBREVIATIONS: 3D, three-dimensional; DMEM, Dulbecco's modified Eagle's medium; FCS, fetal calf serum; PCL, polycaprolactone; PFC, perfluorocarbon; PLGA, poly(lactic-co-glycolic acid).

their own weight. Small hollow structures (e.g., tubes with a small inner diameter) cannot be built without a supporting core. Various strategies to support large hydrogel constructs have been presented.[23,25–27] Shim and co-workers[23] plotted synthetic polymer blends composed of polycaprolactone (PCL) and poly(lactic-co-glycolic acid) (PLGA) to produce a scaffold, which provided mechanical support for the cell-hydrogel mixture that was subsequently injected. Landers and colleagues[25] stabilized a hydrogel structure by dispensing hydrogels or pastes into a bath of a liquid with matching density. Fibrinogen–thrombin and alginate–calcium chloride mixtures have been used to print cell containing constructs layer-by-layer.[26] Immersing the printing platform into alginate solution, for example, stabilized the printed construct by hydrostatic pressure.

Here we employ high buoyant density perfluorocarbons (PFCs) to support less buoyant, soft, and fragile hydrogel constructs, even at very high aspect ratio.[28] PFCs are nontoxic, chemically inert fluids immiscible with water or with oil. Their high oxygen and carbon-dioxide transport ability renders them well suited for submerged cell culture.[29–32] We present a proof-of-concept study demonstrating submerged bioprinting of high aspect ratio, cell-seeded hydrogel structures. In addition, we examined how printing into a high buoyant density liquid impacts precision and size of individually dispensed hydrogel drops compared to printing in air. From a technical point of view, the lowest dispensable drop volume and the correlating drop size as well as the positioning accuracy define the quality of a bioprinter. These parameters determine feature size, shape, and reproducibility that can be achieved. For instance, to print an artificial vein substitute, the minimal drop size and the minimal pattern width, respectively, have to be smaller than the average wall thickness of a naturally occurring human vein (i.e., 50 μm–3 mm).[33] Numerous studies report high-precision printing in air.[34,35] This study describes the printing of soft high-aspect ratio structures in a high buoyant density liquid with respect to positioning precision, drop size, and shape.

Materials and Methods

Hydrogel rod and tube extrusion

Figures 1 and 2 illustrate the supporting effect of submerged bioprinting on hydrogel constructs with a high aspect ratio. Gel rods made of 3% (w/v) agarose were extruded in air and in fluorocarbon (Fluorinert™ Electronic Liquids

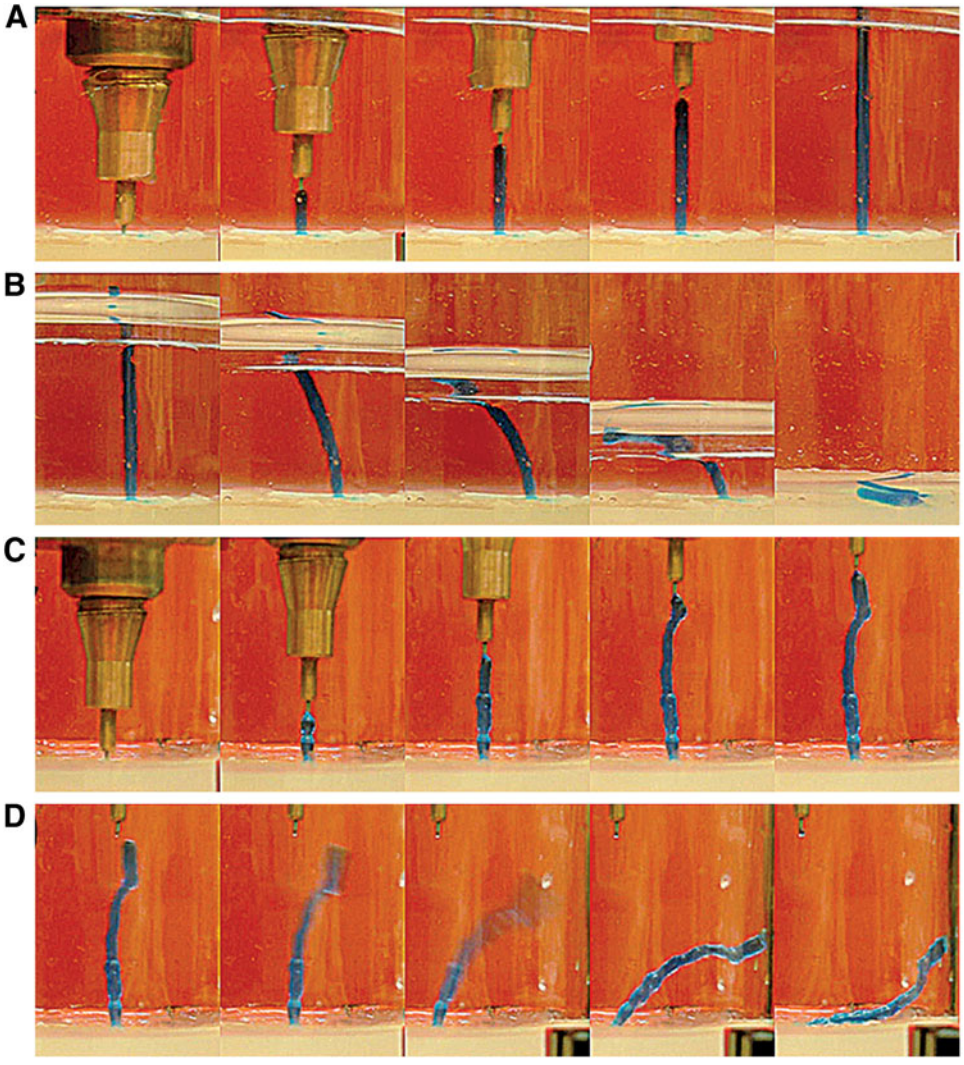

FIG. 1. Submerged hydrogel extrusion in fluorocarbon support fluid. The experiments were conducted with 3% (w/v) agarose stained with methylene blue. **(A)** The extrusion of an agarose rod in fluorocarbon. **(B)** The collapsing of the gel rod upon removal of the support liquid. **(C)** A hydrogel rod extruded in air. **(D)** The rod detaches from the extrusion needle and collapses when a critical height is exceeded.

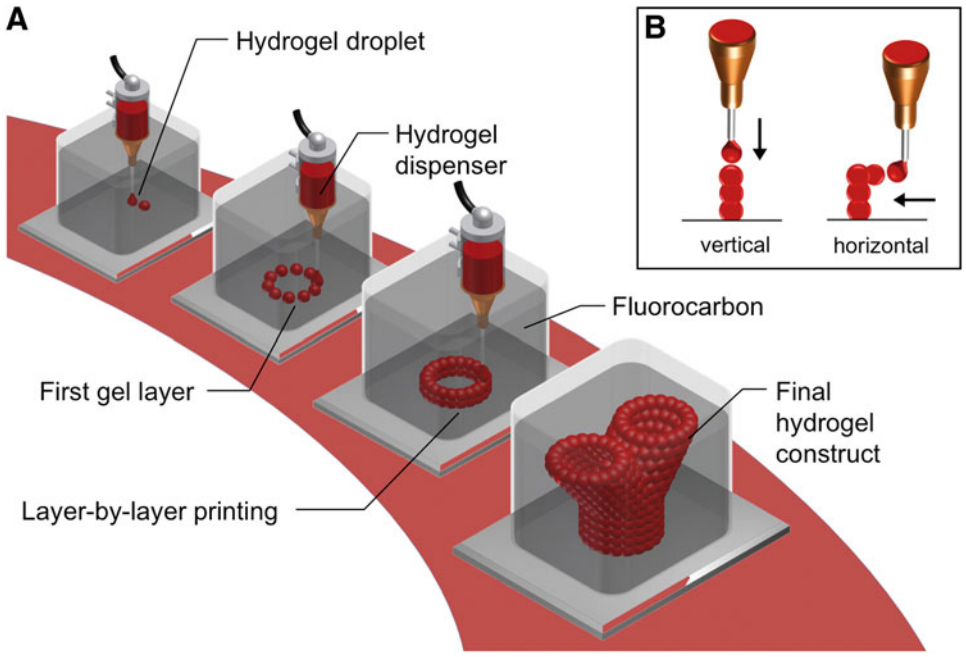

FIG. 2. General concept of submerged bioprinting. **(A)** Single drops of cell laden hydrogel are dispensed layer-by-layer according to a predefined model to form a three-dimensional tissue construct. The printing is performed submerged in a high-density fluorocarbon supporting liquid. **(B)** Hydrogel drops can be appended either vertically or laterally to an existing structure. Due to the buoyant support of the fluorocarbon, branching hydrogel structures or cantilever like constructs can be build without the need for a solid support.

FC-43, 3M Deutschland, Neuss, Germany). The printing process was recorded with a digital video camera attached to a SVM Compact Video Microscope (EO Elektro-Optik Service, Dortmund, Germany). Single frames extracted from the videos are shown.

In addition, we studied cell survival and proliferation in submerged biofabricated, high aspect ratio tubular constructs. Tubes composed of Dulbecco's modified Eagle's medium (DMEM) containing alginate (3%) and L929 mouse fibroblasts (2×10^6/mL) were extruded using a motor-driven syringe with a 5-mm-diameter ring orifice. The solution was extruded vertically against a solid support covered by a thin layer (5 mm) of $CaCl_2$ (50 mg/mL). Upon contact with the $CaCl_2$, the alginate gelled immediately. During alginate extrusion the syringe was retracted while a matching volume of fluorocarbon was simultaneously added to the surrounding container to ensure continuous contact of the retracting orifice with the $CaCl_2$ solution. The lumen of the extruded tube was kept open by injecting fluorocarbon through the inner opening of the ring orifice, thus inflating the tube. The test constructs were completed in <30 sec with an inner diameter of 5 mm, a wall thickness of ~0.1 mm, and a length of up to 3 cm.

Submerged printing platform

The printer used throughout this work was custom built and consisted of a print head mounted on a tri-axially moveable robotic platform. The print head was designed for drop-on-demand printing of cells and hydrogels. The print head comprised a disposable syringe (1 or 5 mL, Terumo® Syringe SS*05SE1 without needle, Terumo, Tokyo, Japan), which was used as gel cartridge, a motor driven plunger, and a dispensing needle (BD Microlance™ 3, 23 G$\times$1.25 inches, no. 14, 0.6 mm$\times$30 mm; Becton, Dickinson and Company, Franklin Lakes, NJ). The syringe had a copper sheet jacket, which was heated by two peltier elements (Standard Peltier-Element 3504, Conrad Electronic SE, Hirschau, Germany), and a digital temperature controller (ENDA ET 1411, Suran Industrieelektronik, Horb, Germany). The printer had four linear drives, a moveable printing platform, and supporting elements from Fischertechnik® (Waldachtal, Germany). Three identical stepper motors with (7.5° rotation per step) were used to move the printer head in X, Y, and Z direction, respectively (no. 82920001 Zwei Phasen Schrittmotor, Crouzet, Hilden, Germany). A fourth linear drive comprising a stepper motor with 1.8° rotation per step controlled the plunger movement (Schrittmotor E547-52500, Emis-Gesellschaft für Electronic und Microprozessorsysteme, Weiden, Germany). The plunger motor was connected to two gears resulting in a 4:1 gear ratio. All linear drives were connected to M4-threaded rods with a slope of 0.7 mm per turn (360°). The printer is shown in Figure 3. The spatial resolution of each of the linear drives is listed in Table 1. The printing platform could be moved 12.4 cm in X- and 7.6 cm in Y-direction. In Z-direction the print head could be moved 5.7 cm. Thus the maximum working volume was 535 cm^3.

Printer control

The stepper motors driving the printing platform and the print head were controlled by two electronic boards (Schrittmotorsteuerkarte SMC800, Emis-Gesellschaft für Electronic und Microprozessorsysteme) powered by a 24-V power supply and connected to a personal computer. Control software was programmed with Visual Basic (Visual Basic 6, Microsoft, Redmond, WA). To implement feedback control of drop deposition, a contact sensor was integrated into the printing system (Fig. 4). The sensor determined whether the needle of the print head touched ground. One electrode serving as ground was connected to the base of the printing platform and covered with an electro-conductive layer of hydrogel (e.g., agarose). The dispenser needle tip served as the second electrode. Both electrodes were connected to an analog-to-digital (A/D) converter (RedLab 1408FS, Meilhaus Electronic, Puchheim, Germany). During printing the voltage between the two electrodes was continuously recorded. When the dispensing needle tip touched the ground electrode or any conductive material that was connected to ground, the electric

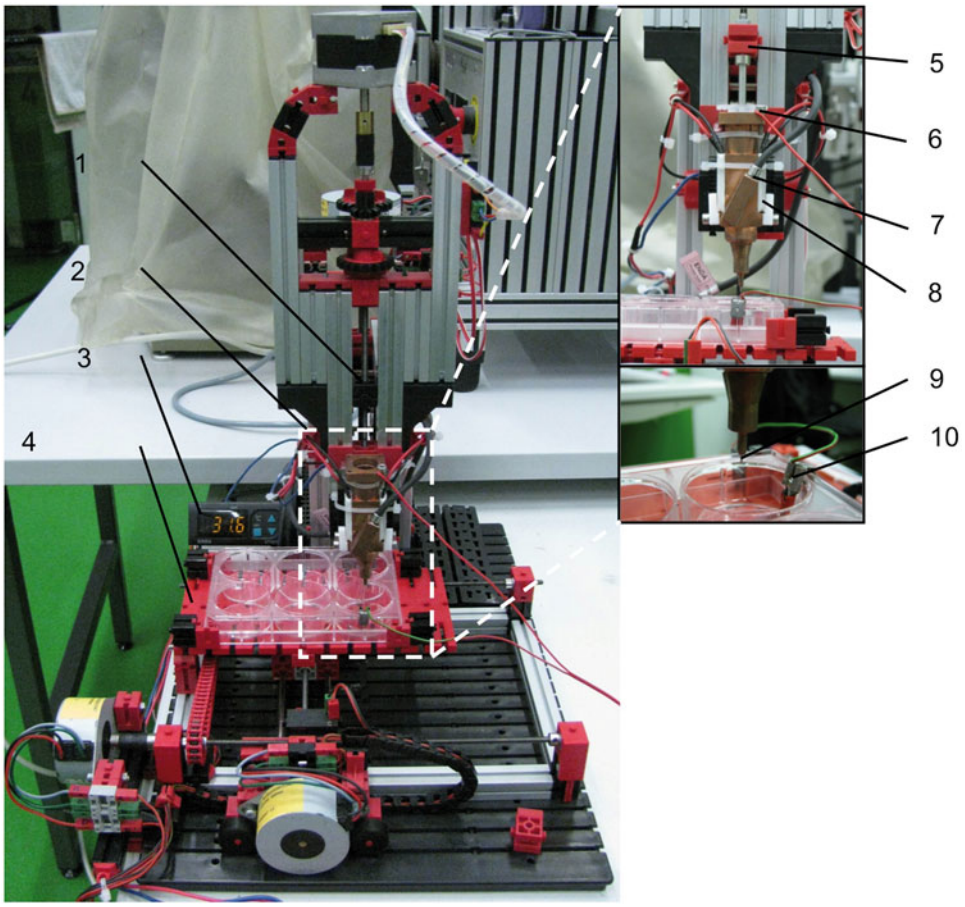

FIG. 3. Bioprinter prototype and its main components. The printer support structure was built from Fischertechnik® components (Waldachtal, Germany). The close-up shows the print head construction in detail. *Legend:* 1, linear drive; 2, print head; 3, temperature controller; 4, printing platform; 5, plunger mounting; 6, print head electrode; 7, temperature sensor; 8, peltier element; 9, printing needle; 10, base electrode.

circuit was closed resulting in a current of $\sim 1.25\,\mu$A. Concomitantly, a voltage drop of 5 V was recorded by the A/D converter. Thus, continuous drop deposition with high accuracy was possible due to the fact that the hydrogel was conductive, but the surrounding fluorocarbon support liquid was not. In summary, the drop deposition process comprised three steps. First, the needle was lowered toward the ground until it touched the substrate or a previously printed layer. Next a drop was expelled at the needle tip. The drop adhered and the needle was retracted.

Lateral drop apposition

To enable the lateral apposition of hydrogel drops and thus the fabrication of delicate overhanging structures, we modified the printing cycle to five steps: print head lowering, drop generation, horizontal drop attachment, print head elevation, and stage repositioning. During printing the printer software stored the position of each drop of the previous layer and calculated its average height. For lateral apposition of hydrogel drops the needle was lowered to align vertically with the stored position of a previously deposited drop. Next a drop was expelled, and the printing stage moved laterally towards the hydrogel structure until the feedback circuit closed and the drop adhered to the bulk structure.

Table 1. Technical Details of XYZ Linear Drives

	X-, Y-, Z-linear drives	*Plunger-drive*
Rotation per step	7.5°	1.8°
Transformation	1:1	1:4
Slope, mm/360°	0.7	0.7
Step width, μm	14.6	0.875

Three identical stepper motors were applied to move the printing platform in the XY-plane, and to lower or lift the print head in Z-direction. The plunger was controlled by a more precise stepper motor.

Hydrogel preparation

We used 3% (w/v) low melting agarose (Biozym Sieve 3:1 Agarose, Biozym Scientific, Oldendorf, Germany) and 3% (w/v) low viscosity alginate (Alginic acid sodium salt, Alfa Aesar, Ward Hill, MA). Agarose and alginate stock solutions were dissolved in water and autoclaved at 121°C for 20 min. The agarose gel was stored at 40°C and was kept at 39°C in the print head. The alginate was stored at 4°C and heated to 36°C before mixing with cells.

Fluorocarbon support liquid (FC-43)

Perfluorotributylamine was purchased from 3M (Fluorinert™ Electronic Liquids FC-43, 3M Deutschland). FC-43 is a colorless and odorless liquid with a density of 1.9 g/cm^3. At 20°C it has a kinematic viscosity of 2.8 mm^2/sec. Its surface tension measures 16 mN/m.

Drop volume range

One step of the plunger motor advanced the plunger by 0.875 μm. Use of a disposable 5-mL syringe with a plunger

diameter of 12.5 mm resulted in a theoretical minimum dispensed volume of 116 nL. To experimentally verify the drop volume, 500 drops of water at 39°C were dispensed and weighed.

Printer performance

The technical performance of the printer was validated by examining drop volume range, dispensing accuracy, and printing speed. The dispensing process was recorded by video microscopy at a magnification of 50× (SVM Compact Video Microscope, EO Elektro-Optik Service). The camera was mounted in an angle of 90° relative to the print head. Recorded images were analyzed using ImageJ software (http://rsb.info.nih.gov/ij/). All experiments were conducted with 3% (w/v) agarose at 39 ± 0.7°C.

Dispensing accuracy

To measure the dispensing accuracy, the lateral offset of a drop relative to the nozzle was measured both after dispensing in air and in FC-43. Four lines of 20 drops each with volumes varying between 116 and 465 nL were printed. The distance between the center of the drops and the nozzle center was measured (Fig. 5A). The positioning deviation Δ was calculated according to Equation 1, where d_N and d_D correspond to the distance between the left border of the evaluation image and the needle or the drop, respectively, and w_N as well as w_D correspond to the needle and drop width, respectively.

$$\Delta = d_N + \frac{1}{2}w_N - \left(d_D + \frac{1}{2}w_D\right) \quad (1)$$

Drop size and shape

To quantify the influence of the supporting liquid on the drop size and shape, we measured the contact angle and the height-to-width ratio of drops printed in air and in FC-43. For each measurement, 20 drops were printed in a row.

Visualization and analysis of printed 3D hydrogel constructs

Printed constructs were photographed using a CCD camera. In addition, the printed constructs were analyzed by computed tomography using a microCT instrument (Tomoscope DUO, CT Imaging, Erlangen, Germany). The instrument was set to 65 kV and 0.38 mA in both X-ray tubes; each flat panel detector acquired 720 projections containing 516 × 506 pixels in 1.1 full rotations within 29 sec; the images were reconstructed with an isotropic voxel size of 52 μm. The images were further processed and viewed with Mimics software (Mimics 14.0, Materialise, Leuven, Belgium).

Cell culture and preparation of cell–hydrogel suspension

For the cell patterning experiments human MG-63 osteosarcoma cells (CRL-1427, American Type Culture Collection, Manassas, VA) were cultured in low glucose DMEM supplemented with 10% fetal calf serum (FCS), 2 mM L-glutamine, 100 U/mL penicillin, and 0.1 mg/mL streptomycin. For printing, 0.5 mL of cell suspension (5×10^6 cells/mL) was mixed with 0.5 mL of melted agarose gel kept at 36°C (± 0.7°C).

For extrusion of cell-laden hydrogel tubes, L929 mouse fibroblasts (CCL-1, American Type Culture Collection) cultured in low glucose DMEM supplemented with 10% FCS and 0.4% gentamycin (10 mg/mL) were mixed with 3% (w/v) alginate. After extrusion the hydrogel tubes were removed from the fluorocarbon container and cultured for up to 7 days in a six-well plate filled with cell culture medium. To prevent the tubes from collapsing, the lumen remained filled with fluorocarbon throughout the culture period.

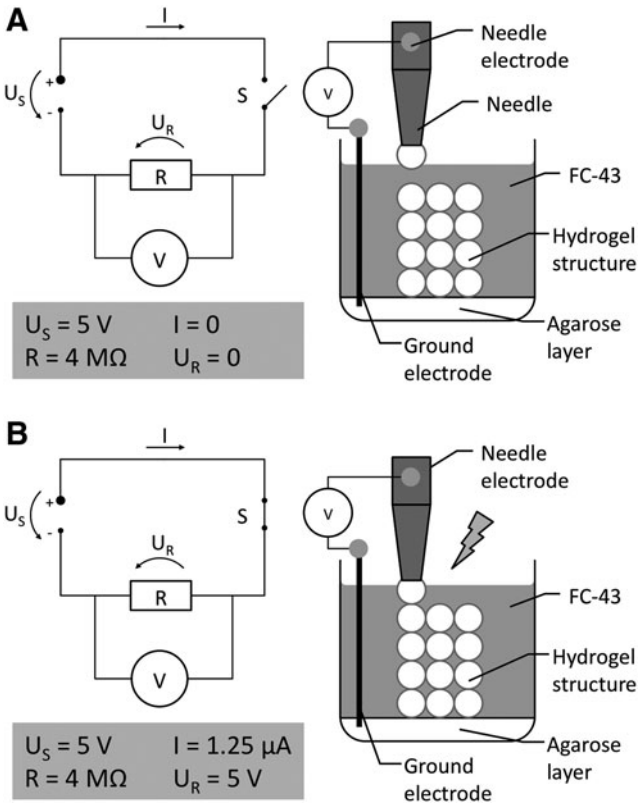

FIG. 4. Function of the electronic drop deposition feedback sensor. The print head needle and the agarose layer at the bottom of the printing vessel were connected to two electrodes. The voltage drop across those electrodes was measured continuously. The sensor exploits the fact that the hydrogel (agarose) is conductive, while the supporting liquid (FC-43) inside the printing vessel is nonconductive. **(A)** As long as the needle or the drop at the needle tip does not touch the agarose ground layer or the preformed hydrogel structure connected to ground, the circuit is open. **(B)** When the needle or the drop at the needle tip touches the preformed structure, the electronic circuit is closed and a voltage drop is recorded. This touch sensor ensures correct drop apposition both in the vertical axis and lateral axis.

Cell viability assay

Cell viability was assessed by live-dead staining using 0.083 mg/mL propidium iodide (P4170-10116, Sigma, Taufkirchen, Germany) and 0.083 mg/mL fluorescein diacetate (F7378-10G Sigma) in Ringer solution. Fluorescence micrographs were recorded using a Leica DMI6000B inverted microscope (Leica Microsystems, Wetzlar, Germany).

Statistical analysis

The data presented in this work represent the mean ± standard deviation. The replicate number n is listed in the respective figure caption. Statistical significance was calculated by

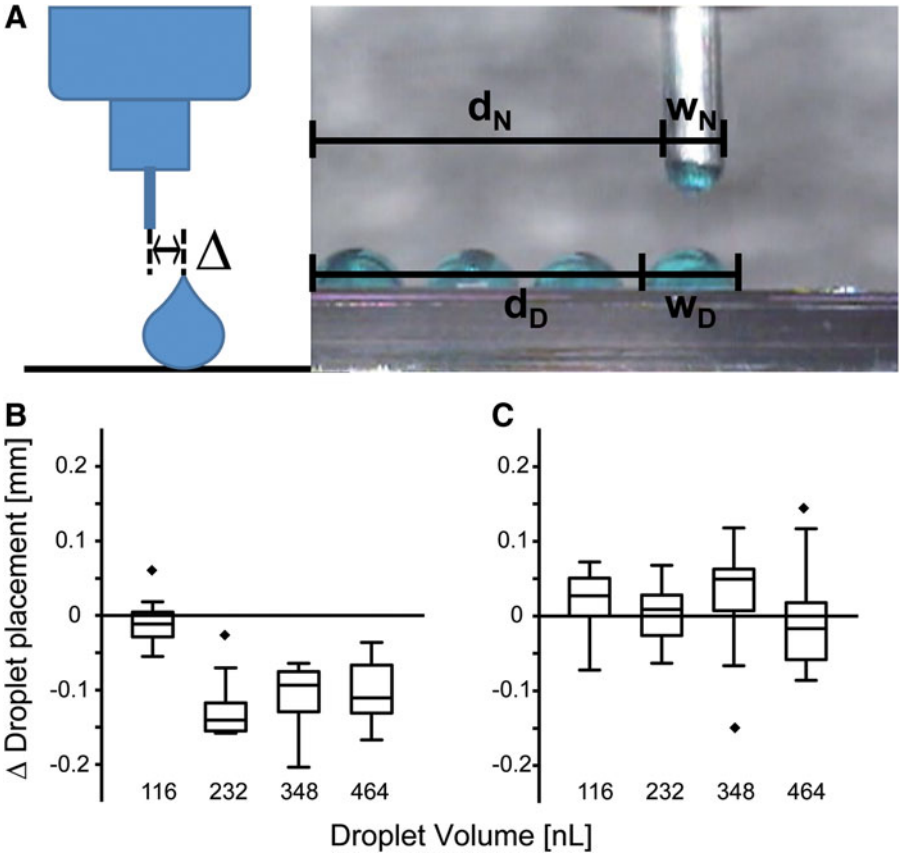

FIG. 5. Dispensing accuracy. **(A)** To assess the accuracy of the dispensing process the offset delta (Δ) from the needle center of a printed drop was measured. Drop diameter was also measured. The dispensing deviation was calculated according to Equation 1. Printing accuracy is given for printing in air **(B)** and for printing in FC-43 **(C)**. Printing accuracy improved in submerged printing. The results are presented in boxplot diagrams, $n = 20$.

one-tailed t-tests. Significance levels were $p < 0.05$, $p < 0.01$, and $p < 0.005$).

Results

Hydrogel rod extrusion

Figure 1 demonstrates that high aspect ratio hydrogel rods could be readily extruded in high-density FC-43 fluorocarbon liquid. Using a syringe and manual deposition of melted agarose, a hydrogel rod of 28-mm length and 1.6-mm thickness with an aspect ratio of 17.5 was made (Fig. 1A). The rod stood stable and upright. The gel rod collapsed immediately when the supporting liquid was removed (Fig. 1B). Hydrogel rods extruded in air were less uniform, bended (Fig. 1C), and likewise collapsed when the rod exceeded 30 mm in length (Fig. 1D).

This simple extrusion experiment demonstrated the major advantage of submerged bioprinting, namely mechanical stabilization of long hydrogel structures with a high aspect ratio. These results prompted us to apply the concept of submerged gel deposition on a 3D freeform fabrication technique, the basic outline of which is shown in Figure 2. Using a dispensing needle, drops of hydrogel were printed into a vessel filled with perfluorocarbon of high buoyant density. 3D hydrogel constructs were printed, layer-by-layer, according to a predefined CAD model. Drops of hydrogel were added on top or lateral to an existing structure (Fig. 2B). Thus, overhanging or branching structures could be printed without a solid support of the protruding edges.

Submerged printing platform

The printer assembly used throughout this study is shown in Figure 3. The spatial resolutions of each of the linear drives are listed in Table 1. The maximum printing platform deflection was 12.4 cm in the X-direction and 7.6 cm in the Y-direction. Z-axis range of the print head was 5.7 cm. The maximum work space was 535 cm^3. Figure 4 illustrates the electrical feedback control of the Z-axis drive. The assembly takes advantage of the fact that unlike aqueous support fluids, perfluorocarbons allow electric feedback control, because they are nonconductive. The printer dispensed volumes between 14.5 and 460 nL. A comparison of calculated and measured drop volume with the respective strokes ranging from 0.9 to 3.5 μm is listed in Table 2. The printing platform could be

Table 2. Droplet Volumes Dispensed at Various Plunger Strokes

Plunger stroke (μm)	*Weight measured (nL)*	*Calculated volume (nL)*
1	88 ± 1	116
2	232 ± 7	232
3	343 ± 11	348
4	458 ± 4	465

Theoretically calculated and experimentally derived values are compared (mean ± SD, $n = 3$).

Table 3. Diameter of Droplets Dispensed on Cell Culture Plastic in Air and in FC-43

Drop volume (nL)	*Diameter in air (mm)*	*Diameter in FC-43 (mm)*
116	0.77 ± 0.03	0.57 ± 0.04
232	0.85 ± 0.02	0.80 ± 0.06
348	0.94 ± 0.03	0.86 ± 0.02
464	1.18 ± 0.01	0.89 ± 0.03

The droplet diameters are listed for four different dispensing volumes (mean ± SD, $n = 5$).

moved with a velocity of 2.75 mm/sec and with an average positioning deviation of 15.43 μm/mm in the X-direction and 17.89 μm/mm in the Y-direction.

Figure 5 illustrates that single drops could be deposited with a lateral accuracy of 11.37 μm in air and 88.74 μm in fluorocarbon. In air, the lateral deposition accuracy was independent of the drop volumes (Fig. 5B). In FC-43 fluorocarbon, droplet deposition accuracy gain at all droplet volumes tested (Fig. 5C).

Submerged single drop deposition

The drop size, the contact angle and the height-to-width ratio of hydrogel drops printed in air and drops printed in FC-43 were analyzed for four different volumes ranging from 116 to 464 nL (Table 3 and Fig. 6). In FC-43 the contact angle and the aspect ratio increased with drop volumes.

Printing complex structures

Using submerged printing and drop deposition we printed hydrogel constructs of complex geometry. We started printing hollow cylinders and overhanging tree structures that would collapse when printed in air. The printing material was agarose. Diameter and height of the hydrogel cylinders could be freely determined. Minimum wall thickness of the constructs was ~0.7 mm achieved by depositing 60-nL drops (Fig. 7A, B). To demonstrate the versatility of submerged printing we printed delicate trees with a trunk thickness of ~1.3 mm (Fig. 7C–F). At a height of 5 mm the trunk branched into five horizontal arms with lengths of ~2.5–4.0 mm, measuring ~0.7 mm in diameter.

Printing vascular bifurcations

Submerged bioprinting was further used to fabricate a 3D model of a vascular bifurcation with a diameter ratio of 1:1 in the common trunk and the two branches, respectively (Fig. 8). The diameter of the trunk was 6.3 mm and the branches measured 6.1 mm, corresponding to the expected a 1:1 ratio. The wall thickness was ~1 mm throughout and the total height of the construct was 10 mm. The bifurcation at 10-mm height was 14 mm wide corresponding to an 80° bifurcation angle. Despite the fact that the construct was fabricated from agarose gel, no solid support was required beneath the branching part of the construct or within its lumen.

Cell patterning

To demonstrate the ability to print living cells, we deposited in agarose MG-63 osteosarcoma cells (Fig. 9). The cells were printed in two layers of 300-μm thickness each, with a lateral resolution of 570 μm. Live-dead staining was performed immediately after printing. The results indicate high cell viability and homogeneous cell distribution. We also showed that cells survived submerged bioprinting for at least 21 days.[28]

Viability of cells cultured in extruded alginate tubes

Viability of cell-laden alginate tubes was analyzed by live-dead staining immediately after printing, and after 1, 4, and 7 days in culture. Figure 10 shows typical micrographs of the tube walls taken with a ×5 lens. The number of cells/colonies present in each photograph is indicated in the lower right insert. The number of cells in a given cell cluster was derived from the cluster volume and the volume of a single cell, which was calculated from the average single-cell diameter. The average diameter d of single cells imaged immediately after extrusion (27 ± 1 μm) was used to calculate the average single-cell volume using the volume function ($d^3\pi/6$). The cluster volume was calculated accordingly, and divided by the single cell volume. Three parts of the tube wall, each representing a volume slice of 0.1 μL ($1 \times 1 \times 0.1$ mm^3) were evaluated. Immediately after fabrication of the gel tubes, 292 ± 12 viable and 13 ± 5 dead cells were counted in a typical 0.1-μL wall segment (96% viability). One day after fabrication the number of viable cells increased to 452 ± 38, while the number of dead cells rose to 17 ± 3 cells (96% viability). At day four, 210 cell clusters with an average of 4.42 cells per cluster were counted resulting in 928 ± 213 viable and 12 ± 3 dead cells (99% viability). At day seven, 153 cell clusters were counted, comprising 7.8 cells on average. Hence, the final number of viable cells increased to 1196 ± 53. At the same time 37 ± 13 dead cells were counted (97% viability).

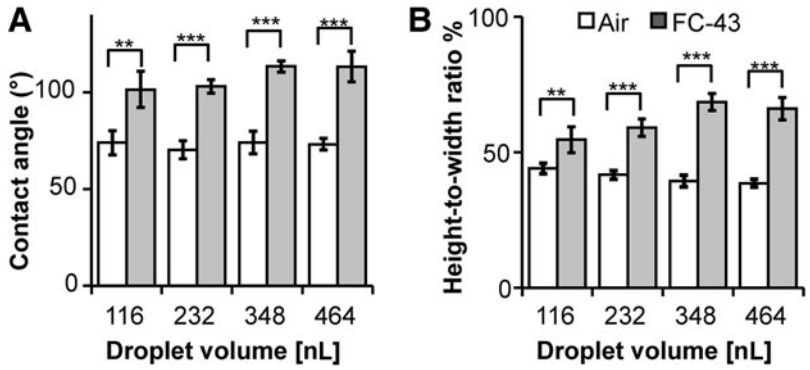

FIG. 6. Drop shape in submerged printing versus air printing. **(A)** Contact angle and **(B)** height-to-width ratio measurements of drops printed in air as well as in fluorocarbon (FC-43). The graphs illustrate mean ± SD, $n = 5$. ***$p < 0.001$, **$p < 0.01$.

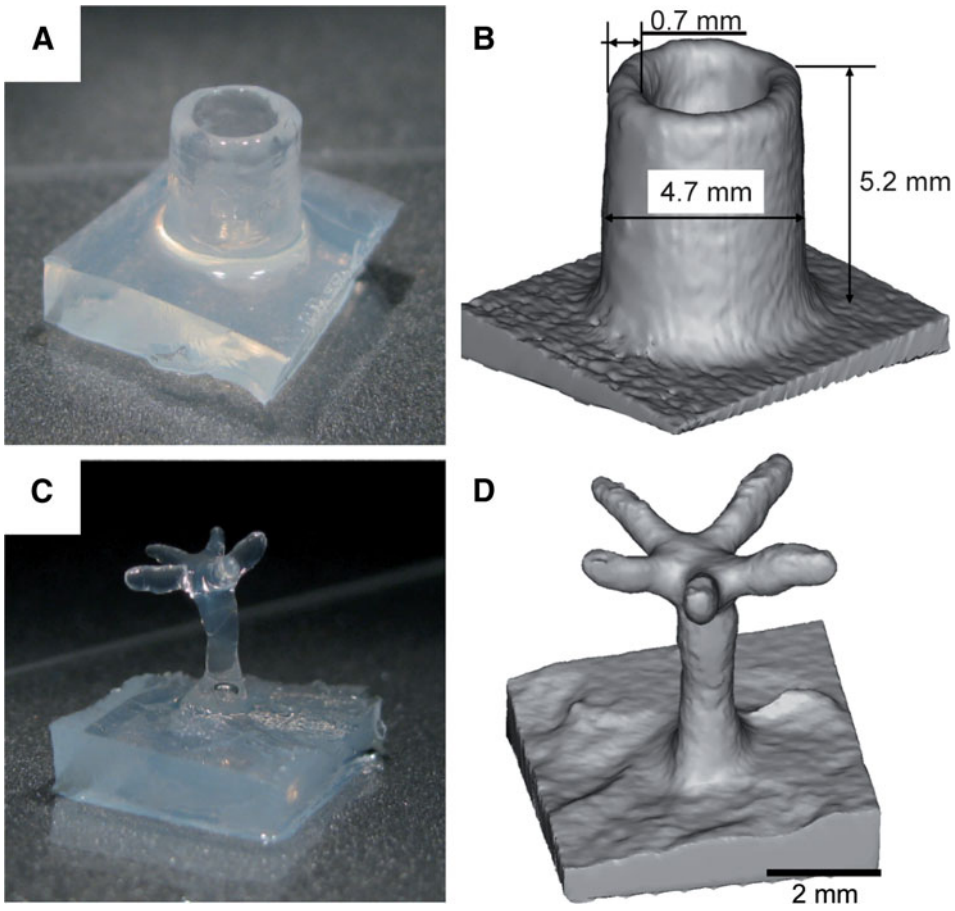

FIG. 7. Submerged printing of hollow and delicate overhanging structures. **(A)** Photograph and **(B)** computed tomography (CT) image of an agarose cylinder. The CT data were used to determine the dimensions of the printed objects. The photographs illustrate their visual appearance. **(C)** Photograph and **(D)** CT image of a delicate tree structure (scale bar, 2 mm).

Figure 10 thus shows that cells grew vigorously and formed clonal colonies within the 7-day culture. At day 1, the cells underwent crisis, as would be expected from a starting cell culture, in that slightly elevated numbers of dead cells were observed. At day 4, clonal growth was most vigorous with almost no dead cells. At day 7, the cells had formed large clusters with an average diameter of $54 \pm 3\,\mu$m. The largest clusters of $\sim$90-μm diameter had a necrotic core suggesting nutrient depletion. In summary this experiment showed that submerged extrusion of alginate under fluorocarbon sustained vigorous cell growth up to 1 week even without perfusion/percolation of the hollow structures, which should further improve the culture success.

Discussion

Perfluorocarbons as liquid support

We demonstrate the printing of hydrogels submerged in high-density perfluorocarbon support fluid. Large, high aspect ratio structures could be readily manufactured by simple extrusion of hydrogels. Branching structures with overhang were likewise produced with the aid of liquid support of PFC (e.g. FC-43). Besides its function in supporting high aspect ratio structures, printing in high-density PFC affected drop size and shape, too. The agarose drops printed in FC-43 had a higher contact angle, were less flattened, and thus had a smaller diameter than drops with equal volume printed

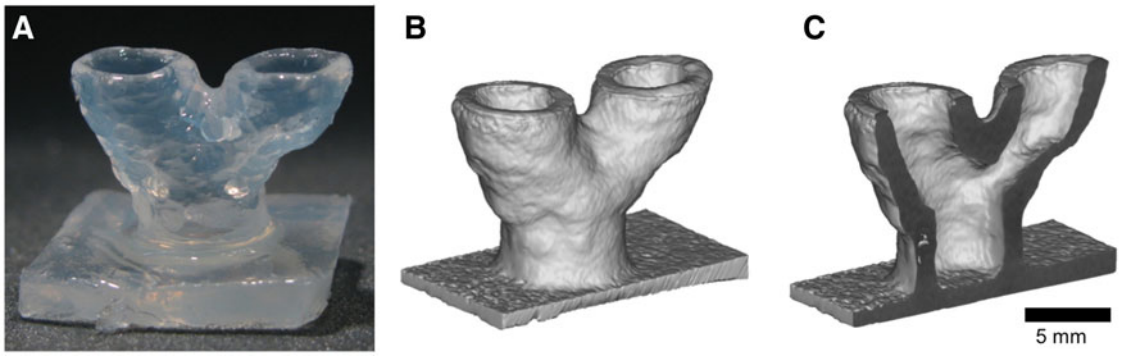

FIG. 8. Submerged printing of an arterial bifurcation. **(A)** Photograph of the bifurcation model. **(B)** and **(C)** CT images of the construct in full and in sectional view (scale bar, 5 mm).

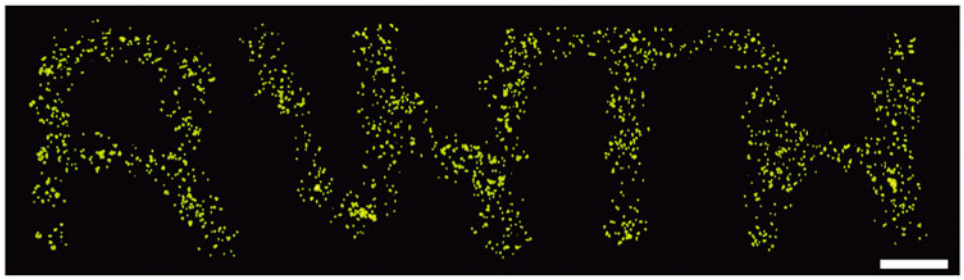

FIG. 9. Submerged bioprinting of live cells. MG-63 osteoblastic cells encapsulated in agarose were printed onto a solid support submerged in PFC. Live-dead staining was performed after printing demonstrating that all cells survived the printing process (scale bar, 1 mm).

in air (Table 3 and Fig. 6). Hence, submerged printing inherently improved the spatial resolution of the printer. The increased contact angle and reduced flattening of the drops were probably caused by a combination of three factors: the hydrophobicity of the supporting fluid, a reduced adhesion between hydrogel-needle tip and hydrogel-print surface, and the increased buoyant lift of the drop in PFC versus air. Minimum drop size in this work was ~100 nL. Much smaller drops and thus increased lateral resolution should become possible by connecting commercial nanoliter dispensing systems to the printer.

Overhanging structures without solid support

Current drop-on-demand bioprinters usually dispense drops of hydrogel by ink-jet technology, microvalves, or drop ejection attaining high precision drop volumes in the picoliter to nanoliter range.[24,26,34–36] Overhanging structures may be produced by printing into an absorptive, solidifying support and removing the unreacted support material after completion of the printing process. With the drop-dispensing process described in this work, drops in the nano- to microliter range were generated and precisely deposited using a simple disposable needle. Precise control of the drop positioning was achieved by integrating a contact sensor at the needle tip. This technique allowed drops to be deposited with high precision both vertically and laterally.

Fabrication of high aspect ratio gel structures

Bioprinting studies commonly report fabrication of microscopic hydrogel structures or planar single layer constructs.[20,24,34,36,37]

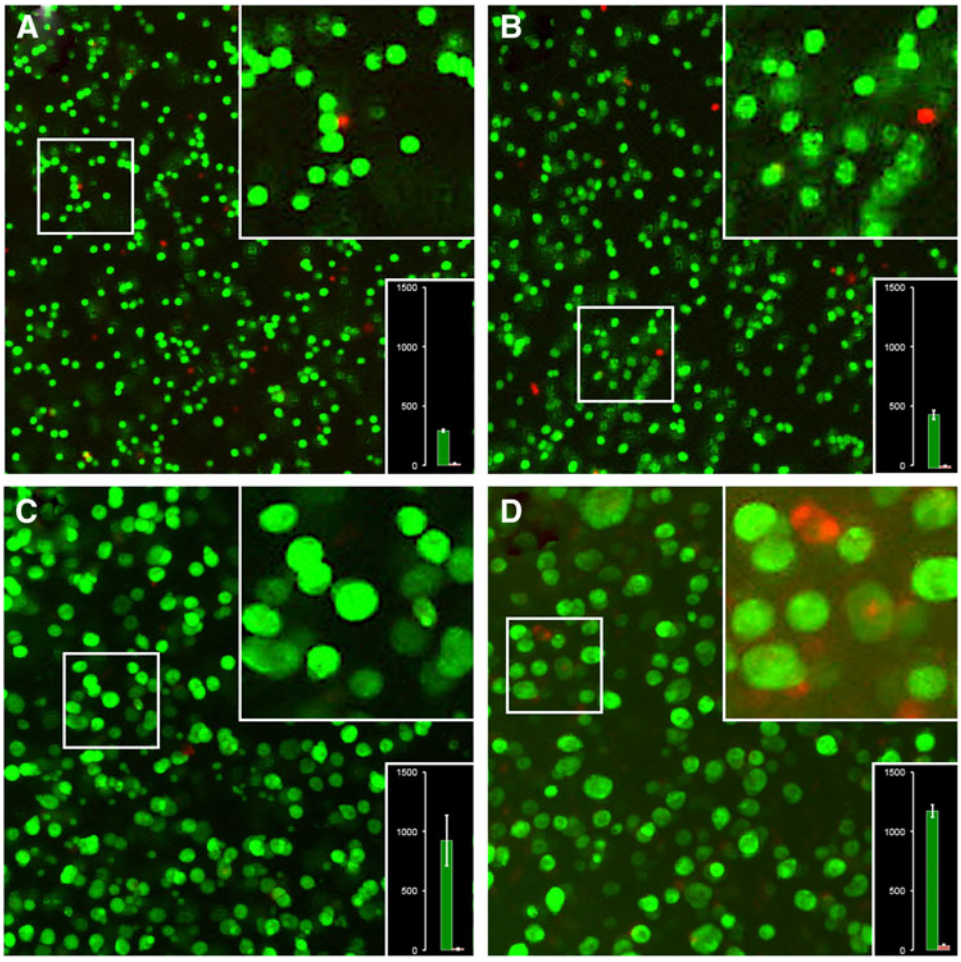

FIG. 10. Cell viability and proliferation in submerged biofabricated alginate tubes. Micrographs of L929 cells and cell clusters in extruded alginate tubes 1 hr **(A)**, 1 day **(B)**, 4 days **(C)**, and 7 days **(D)** after extrusion. Each panel shows an overview taken with a ×5 lens, an insert with magnified cells and a bar graph showing the number of viable and dead cells or cell clusters. Cell-laden alginate tubes were extruded using a syringe with a 5-mm-diameter ring orifice. Cell concentration was adjusted to 2×10^6/mL in 3% alginate solution. Tubes with a length of up to 3 cm, 5-mm outer diameter, and ~0.1-mm wall thickness were manufactured. The extruded hollow tubes were supported by perfluorocarbon both inside and outside the lumen. Cells were grown for up to 1 week. For image recording the cell-laden tubes were re-oriented along their long axis in a petri dish and live-dead staining was performed.

Several authors specifically mentioned the difficulty in building high aspect structures made of hydrogel.[23,27,35] For instance, Lee and colleagues[35] printed collagen hydrogel scaffolds with fluidic channels up to 1.45 mm thick. According to the authors, thicker structures would have required additional mechanical support.[35] Shim and colleagues[23] concluded that maintaining the 3D shape of a printed structure consisting of pure hydrogel is difficult due to weak mechanical stability. The authors therefore designed hybrid scaffolds composed of synthetic biomaterials (e.g., PCL/PLGA blends), which served as an integral support structure, and natural hydrogel (e.g., collagen), which added functionality. Other studies fabricated large hydrogel structures using alginate hydrogels either pre-mixed with $CaCl_2$,[38] plotted into a bath of $CaCl_2$,[25] or by printing $CaCl_2$ solution into an alginate solution.[26] Through use of these techniques, hydrogel constructs of similar size and shape to the ones shown here were created. Submerged bioprinting differs, however, in that the supporting liquid has higher density than the printed material. The density difference supports long and tubular structures of even very high aspect ratio. In addition, the PFC support liquid is biocompatible and has high oxygen and carbon-dioxide transport capacity rendering it ideal for use with living cells.[29] Thus submerged bioprinting in PFC should also allow time-consuming printing tasks, when oxygen supply and removal of CO_2 during the printing process might become limiting.

Prospective improvements

Throughout this pilot study we used agarose hydrogels. Compared to other hydrogels this is a rather stiff material. In addition, unlike biomimetic hydrogels such as peptide amphiphiles or protein-based hydrogels such as collagen, fibrinogen, or elastin, agarose does not promote cell adhesion.[39,40] Even though agarose gels can be modified to better promote cell development, further experiments must prove that submerged printing is suitable for other types of hydrogels as well. Besides material-related challenges, the printing system requires further refinement. Printing resolution, accuracy, and the speed should, however, be readily enhanced by switching from the low-cost components used in this study to high performance commercial components.

Possible application of submerged bioprinting for printing vascular grafts

We foresee first applications of submerged bioprinting in vascular tissue engineering. Here, we extruded into liquid support PFC, high aspect ratio cylindrical structures measuring 3 cm in length that are very difficult to produce otherwise. Cylinders with an inner diameter of 2.9 mm and a wall thickness of 0.65 mm were likewise printed using a drop-on-demand syringe print head. Taken together, these constructs are similar in size to small-bore vascular grafts that are routinely used to replace stenotic arteries in vascular surgery.[33] Furthermore, submerged bioprinting may be even suitable to produce branching structures typical of vascular bifurcations (Figs. 7 and 8).

Acknowledgments

The authors thank Fabian Kiessling and Twan Lammers, RWTH Aachen, for microCT use, and Yu Pan, RWTH Aachen, for fluorescence microscopy.

Author Disclosure Statement

A.B., D.F.D.C., M.W., S.N., H.F., and W.J.-D. are named inventors on a patent application of RWTH Aachen University. B.T. declares no competing financial interests exist.

References

1. Vacanti C, Vacanti JP. The science of tissue engineering. Orthop Clin North Am. 2000;31:351–356.
2. Griffith LG, Naughton G. Tissue engineering—current challenges and expanding opportunities. Science. 2002;295:1009–1014.
3. Choi NW, Cabodi M, Held B, et al. Microfluidic scaffolds for tissue engineering. Nat Mater. 2007;6:908–915.
4. Rastegar F, Shenaq D, Huang J, et al. Mesenchymal stem cells: molecular characteristics and clinical applications. World J Stem Cells. 2010;2:67–80.
5. Boucard N, Viton C, Agay D, et al. The use of physical hydrogels of chitosan for skin regeneration following third-degree burns. Biomaterials. 2007;28:3478–3488.
6. Chen G, Sato T, Ushida, et al. Tissue engineering of cartilage using a hybrid scaffold of synthetic polymer and collagen. Tissue Eng. 2004;10:323–330.
7. Malda J, Klein TJ, Upton Z. The roles of hypoxia in the in vitro engineering of tissues. Tissue Eng. 2007;13:2153–2162.
8. Rouwkema J, Rivron NC, van Blitterswijk C. Vascularization in tissue engineering. Trends Biotechnol. 2008;26:434–441.
9. Boland T, Mironov V, Gutowska A, et al. Cell and organ printing 2: fusion of cell aggregates in three-dimensional gels. Anat Rec A Discov Mol Cell Evol Biol. 2003;272:497–502.
10. Varghese D, Deshpande M, Xu T, et al. Advances in tissue engineering: cell printing. J Thorac Cardiovasc Surg. 2005;129:470–472.
11. Mironov V, Boland T, Trusk T, et al. Organ printing: computer-aided jet-based 3D tissue engineering. Trends Biotechnol. 2003;21:157–161.
12. Mironov V, Reis N, Derby B. Bioprinting: a beginning. Tissue Eng. 2006;12:631–634.
13. Sachlos E, Czernuszka JT. Making tissue engineering scaffolds work. Review: the application of solid freeform fabrication technology to the production of tissue engineering scaffolds. Eur Cell Mater. 2003;5:29–39.
14. Pham DT, Dimov SS. *Rapid Manufacturing: The Technologies and Applications of Rapid Prototyping and Rapid Tooling*. Springer-Verlag: London, 2001.
15. Fedorovich NE, Alblas J, de Wijn JR, et al. Hydrogels as extracellular matrices for skeletal tissue engineering: state-of-the-art and novel application in organ printing. Tissue Eng. 2007;13:1905–1925.
16. Geckil H, Xu F, Zhang X, et al. Engineering hydrogels as extracellular matrix mimics. Nanomedicine. 2010;5:469–484.
17. Burdick JA. Bioengineering: cellular control in two clicks. Nature. 2009;460:469–470.
18. Tibbitt MW, Anseth KS. Hydrogels as extracellular matrix mimics for 3D cell culture. Biotechnol Bioeng. 2009;103:655–663.
19. Lee KY, Mooney DJ. Hydrogels for tissue engineering. Chem Rev. 2001;101:1869–1879.
20. Khoda KM, Ozbolat IT, Koc B. A functionally gradient variational porosity architecture for hollowed scaffolds fabrication. Biofabrication. 2011;3:034106.
21. Tse JR, Engler AJ. Preparation of hydrogel substrates with tunable mechanical properties. In: *Current Protocols in Cell*

Biology 47. Bonifacino JS, Dasso M, Harford JB, Lippincott-Schwartz J, Yamada KM (eds.) John Wiley: New York, NY; pp. 10.16.1–10.16.16; 2010.
22. Park JH, Chung BG, Lee WG, et al. Microporous cell-laden hydrogels for engineered tissue constructs. Biotechnol Bioeng. 2010;106:138–148.
23. Shim J-H, Kim JY, Park M, et al. Development of a hybrid scaffold with synthetic biomaterials and hydrogel using solid freeform fabrication technology. Biofabrication. 2011;3: 034102.
24. Moon S, Hasan SK, Song YS, et al. Layer by layer three-dimensional tissue epitaxy by cell-laden hydrogel drops. Tissue Eng Part C Methods. 2010;16:157–166.
25. Landers R, Pfister A, Hübner U, et al. Fabrication of soft tissue engineering scaffolds by means of rapid prototyping techniques. J Mater Sci. 2002;7:3107–3116.
26. Boland T, Tao X, Damon BJ, et al. Drop-on-demand printing of cells and materials for designer tissue constructs. Mater Sci Eng C. 2007;27:372–376.
27. Shim J-H, Lee J-S, Kim JY, et al. Bioprinting of a mechanically enhanced three-dimensional dual cell-laden construct for osteochondral tissue engineering using a multi-head tissue/organ building system. J Micromech Microeng. 2012;22:085014.
28. Duarte Campos D, Blaeser A, Weber M, et al. Three-dimensional printing of stem cell-laden hydrogels submerged in a hydrophobic high-density fluid. Biofabrication. 2013;5:015003.
29. Juszczak MT, Elsadig A, Kumar A, et al. Use of perfluorodecalin for pancreatic islet culture prior to transplantation: a liquid-liquid interface culture system-preliminary report. Cell Transplant. 2011;20:323–332.
30. Lowe KC, Davey MR, Power JB. Perfluorochemicals: their applications and benefits to cell culture. Trends Biotechnol. 1998;16:272–277.
31. Lowe KC. Perfluorochemical respiratory gas carriers: benefits to cell culture systems. J Fluor Chem. 2002;118: 19–26.
32. Rappaport C. Review—progress in concept and practice of growing anchorage dependent mammalian cells in three dimension. In Vitro Cell Dev Biol Anim. 2003;39:187–192.
33. Tortora GJ, Nielsen MT. The cardiovascular system: blood vessels. In: *Principles of Human Anatomy*, 11th edition. Wiley: Hoboken, NJ; 2008, pp. 481–540.
34. Nakamura M, Kobayashi A, Takagi F, et al. Biocompatible inkjet printing technique for designed seeding of individual living cells. Tissue Eng. 2005;11:1658–1666.
35. Lee W, Lee V, Polio S, et al. On-demand three-dimensional freeform fabrication of multi-layered hydrogel scaffold with fluidic channels. Biotechnol Bioeng. 2010;105:1178–1186.
36. Cui X, Boland T. Human microvasculature fabrication using thermal inkjet printing technology. Biomaterials. 2009;30: 6221–6227.
37. Song S-J, Choi J, Park Y-D, et al. A three-dimensional bioprinting system for use with a hydrogel-based biomaterial and printing parameter characterization. Artif Organs. 2010;34:1044–1048.
38. Cohen DL, Malone E, Lipson HOD, et al. Direct freeform fabrication of seeded hydrogels in arbitrary geometries. Tissue Eng. 2006;12:1325–1335.
39. Khaing ZZ, Schmidt CE. Advances in natural biomaterials for nerve tissue repair. Neurosci Lett. 2012;519:103–114.
40. Matson JB, Stupp SI. Self-assembling peptide scaffolds for regenerative medicine. Chem Commun. 2012;48:26–33.

Address correspondence to:
Willi Jahnen-Dechent, PhD
Helmholtz Institute of Biomedical Engineering,
Biointerface Laboratory
RWTH Aachen University Hospital
Pauwelsstrasse 30
52074 Aachen
Germany

E-mail: willi.jahnen@rwth-aachen.de